

Formation of impurity bands in doped semiconductors

J. Monecke, J. Kortus, and W. Cordts

Department of Physics, Mining Academy of Freiberg, B.-v.-Cotta-Strasse 4, 0-9200 Freiberg, Germany

(Received 31 August 1992)

The determination of the widths and energetic positions of impurity bands in doped semiconductors has been performed in the past by band-structure calculations of hypothetical impurity superlattices or by applying multiple-scattering theories (e.g., the Klauder-V approximation) with essentially different results. The related problems of ionization energies in dense plasmas and of exciton ionization energies in highly excited semiconductors have additionally been treated using two-particle Green's-function techniques with the result of vanishing bandwidths with vanishing temperature for all densities below the Mott value. The reasons for these differences are discussed and the widths of impurity bands in doped semiconductors are calculated by the Wigner-Seitz method and a multiple-scattering approximation, which is correct to first order with respect to the impurity concentration.

I. INTRODUCTION

The calculation of impurity bands in doped semiconductors is a complicated problem which requires, in principle, the combined solution of the following problems.

(1) The bare potential of one impurity in the host semiconductor (e.g., of Si on a Ga site in GaAs) must be given.

(2) The screening of the bare potential by the presence of all other impurities and the free carriers, respectively, must be known.

(3) The formation of impurity bands for a constant density of impurities has to be calculated.

(4) The formation of band tails by density fluctuations has to be investigated.

(5) Apart from the screening of the bare potential "real" many-body effects such as the formation of a D^- band and possible spin- and charge-density fluctuations in a frustrated ground state have to be taken into account.

Closely related problems are those of the determination of the density-dependent energies and widths of spectral lines in dense plasmas and the formation of exciton bands in highly excited semiconductors, in which cases the heavier charge carriers are allowed to move.

In this contribution our main emphasis is on determining the formation of impurity bands for a constant density of impurities without fluctuations. We shall restrict ourselves to the effective-mass approximation, treating the host semiconductor as a homogeneous medium with a dielectric constant ϵ and the charge carriers as free particles with an effective mass m^* . Bare potentials are approximated to be of pure Coulomb type. The coupling of different bands of the host semiconductor by the impurities as well as impurity core effects thus are neglected.

The screening of bare Coulomb potentials by other polarizable neutral impurities in the low-density limit and by charge carriers in the high-density limit is a complicated problem, which has been handled with different degrees of sophistication.¹⁻⁴ The best static screening the-

ory available now is to calculate screened potentials self-consistently, as was done for disordered solids by Vignale *et al.*^{5,6} by combining the coherent potential approximation with the local-density approximation.

In the case of dense plasmas and of highly excited semiconductors the screening of bare potentials has been treated by means of two-particle Green's functions, taking into account the dynamic screening of the Coulomb potential and dynamic single-particle self-energies in the same approximation.⁷⁻⁹ The main emphasis was the determination of the absolute values of the energy positions of both the analog of the conduction-band edge and the impurity level, which means of the so-called Debye shift which is of importance for the proper description of thermodynamics.¹⁰ The result was a vanishing impurity (or bound-state or exciton) bandwidth with a vanishing temperature for all densities below the Mott one, defined by the bound state merging with the continuum. The reason for this deficiency is that the hopping of an electron between the impurities (or between the ions or holes) was not taken into account explicitly in the approximate two-particle Green's function. The other impurities (ions or holes) and the other electrons beside the considered pair contributed only to screening. Therefore, no band formation could be obtained.

In this contribution we shall restrict ourselves to the simple Thomas-Fermi screening approximation. It gives the correct high-density limit as well as the correct limit at vanishing impurity density. For small impurity densities the Thomas-Fermi screening obviously is too large. We want, however, to compare our results with those obtained by Serre and Ghazali¹¹ and, therefore, chose the same starting point.

The density of states of impurity bands in the approximation of a nonfluctuating impurity density shows sharp cutoffs and no band tails. Band tails can be obtained either by the optimum fluctuation method¹²⁻¹⁴ or by the more simplified method of Serre, Ghazali, and Leroux Hugon,¹⁵ additionally.

“Real” many-body problems such as the formation of a D^- band and a nondegenerate (according to the third law of thermodynamics) ground state with spin- or charge-density waves in a frustrated disordered impurity lattice¹⁶⁻¹⁹ are beyond the scope of this paper and will not be considered.

The problem we shall be concerned with is the density dependence of impurity bands in the case of non-fluctuating potentials. The earliest attempts in this direction were Wigner-Seitz calculations²⁰ of hypothetical impurity superlattices carried out by Baltensperger,²¹ Mott and Davies,¹⁶ and Bhatt and Rice.¹⁷ In all these calculations bare Coulomb potentials were used. We shall, therefore, first repeat them in Sec. II for Thomas-Fermi screened (Yukawa-type) potentials in order to obtain lower limits for the widths of impurity bands, supposing that ordered impurity arrays give smaller bands in comparison with disordered ones.

The standard method to treat disorder (without taking into account density fluctuations) is the well-known self-consistent coherent potential approximation.^{22,23} Until now it could be applied to the present case of long range and, hence, overlapping impurity potentials,¹¹ though the recent extension of the multiple-scattering theory to space-filling potentials²⁴ may lead to a corresponding generalization of the coherent potential approximation.

As early as 1961 Klauder²⁵ proposed a simplified version of the coherent potential approximation, the Klauder-V approximation, in which so-called multiple-occupancy corrections are neglected which should be tolerable at usual impurity concentrations. The much easier self-consistent Born approximation,^{26,27} the Klauder-III approximation, does not result in impurity bands at all and can be used in the high-density limit only. The Klauder-V approximation was first applied by Serre and Ghazali¹¹ to the problem of impurity band formation in the three-dimensional case. Later it was used by Gold, Serre, and Ghazali²⁸ in the case of a two-dimensional impurity arrangement as was realized in a sodium-doped Si metal-oxide-semiconductor field-effect transistor. The result of Ref. 11 is an impurity bandwidth which for typical densities ($N_D \sim 0.05$ in the notation of Ref. 11) is about 25 times larger than that obtained from Wigner-Seitz calculations and which is much broader than found experimentally (see, e.g., Ref. 29), resulting in a Mott density which is about ten times smaller than the experimental one.

Serre and Ghazali¹¹ tried to trace back this large impurity bandwidth to the enhanced Thomas-Fermi screening. Here, we adopt another point of view. We believe the Wigner-Seitz calculations with the bare and Thomas-Fermi screened Coulomb potentials to prove that screening enhances the impurity bandwidth, however, not to the magnitude obtained in Ref. 11. We trace back the enhanced bandwidth of Serre and Ghazali to another reason.

In Ref. 30 it was proved in the case of δ -like potentials that self-consistent theories such as the coherent potential approximation or the Klauder-V approximation correctly reproduce the self-energy $M|_{c=0}$ in the limit of a vanishing impurity concentration c , as is well known, but

not its first derivative with respect to the concentration $\frac{dM}{dc}|_{c=0}$ at energies close to that of bound states. The same is true in all cases of effective-medium approximations, such as in the case of the Bruggeman theory for the effective dielectric constant of a composite close to the frequency of a possible Fröhlich mode.³¹ Because the first derivative $\frac{dM}{dc}|_{c=0}$ is responsible for the imaginary part of M for small c , an error in this produces a wrong density of states in the limit of small c , although the result for $c \equiv 0$ is correct. This was demonstrated in Ref. 30 to produce a strongly enhanced impurity bandwidth in the case of δ -like impurity potentials and will be shown in this paper to result in the same effect for a Thomas-Fermi screened Coulomb potential. We, therefore, will use a correct linear approximation $M = M|_{c=0} + c \frac{dM}{dc}|_{c=0}$ for the calculation of impurity bands, which is applicable for the small impurity concentrations of interest in doped semiconductors.

In order to be definite we shall treat an n -type direct semiconductor with shallow donors as impurities and electrons as charge carriers in the following.

In this paper first we perform Wigner-Seitz calculations of impurity bands with bare and Thomas-Fermi screened Coulomb potentials. After an outline of the multiple scattering approach in Sec. III we will present in Sec. IV the reasons why we prefer a linear concentration approximation against a self-consistent one for the present problem. Results will be presented in Sec. V and the conclusions are given in Sec. VI.

II. WIGNER-SEITZ CALCULATION OF IMPURITY BANDS

The first and easiest structure-independent method for an energy-band calculation is the Wigner-Seitz method,²⁰ which was applied to the calculation of concentration-dependent impurity bands in semiconductors by Baltensperger,²¹ Mott and Davies,¹⁶ and Bhatt and Rice¹⁷ for bare Coulomb impurity potentials. It will be applied here to unscreened Coulomb and Thomas-Fermi screened Coulomb potentials.

The basic assumption of the Wigner-Seitz method is that around each (screened or unscreened) donor there is exactly one electron in order to ensure charge neutrality, so that the combined effect of all other impurities with their neutralizing electrons is nearly zero at a given ion. This assumption can be justified by the fact that (in the case of Coulomb potentials) the Madelung numbers of regular impurity lattices (e.g., $-1.760122/r_s$, $-1.791749/r_s$, and $-1.791861/r_s$ for simple cubic, fcc, and bcc lattices³²) all are close to the value $-1.8/r_s$ of the Wigner-Seitz approximation. The Wigner-Seitz radius r_s is defined as usual by $\frac{4\pi}{3}(r_s a_B)^3 c = 1$, where c is the donor concentration and a_B is the effective Bohr radius

$$a_B = \frac{\hbar^2 \epsilon}{m^* e^2} = \frac{e^2}{2\epsilon E_D}$$

with E_D being the ground-state binding energy

$$E_D = \frac{m^* e^4}{2\epsilon^2 \hbar^2}$$

of a single impurity.

In the case of a random donor distribution and a constant electron density the Madelung number vanishes (see, e.g., Ref. 33). At first glance this seems to disprove the applicability of the Wigner-Seitz method to the present problem. The electron density, however, is not constant at all. Due to the requirement of local charge neutrality the electron density over large scales will be locally equal to the fluctuating ion density, and we can suppose that each ion is neutralized by exactly one electron.

The small-scale electron distribution around each ion, then, can be calculated with the help of the Wigner-Seitz method. It gives rise, in principle, to a self-consistent potential, which is approximated here by the Thomas-Fermi screened Coulomb potential.

The Wigner-Seitz method requires for s states the solution of the radial Schrödinger equation

$$\frac{d^2\varphi}{dr^2} + \frac{2}{r} \frac{d\varphi}{dr} + [E + V(r)]\varphi = 0, \quad (1)$$

with $V(r) = \frac{2}{r}$ for the unscreened Coulomb potential and $V(r) = \frac{2}{r} e^{-k_{FT}^2 r}$ with $k_{FT}^2 = 4\sqrt{\frac{9}{4\pi^2} r_s^{-1}}$ for the Thomas-Fermi screened one, inside a sphere of radius r_s with the boundary conditions $\frac{\partial\varphi}{\partial r}|_{r_s} = 0$ for the band bottom and $\varphi|_{r_s=0} = 0$ for the top of the band. We have chosen effective length and energy units so that $a_B = 1$ and $E_D = -1$. The solution of (1) was obtained numerically by the Runge-Kutta method of fourth order. The result (for the lowest impurity band corresponding to $1s$ states for $r_s \rightarrow \infty$) is plotted in Fig. 1 for both potentials.

In the Coulomb case the result is identical with those of Refs. 16, 17, and 21. The impurity band in the Thomas-

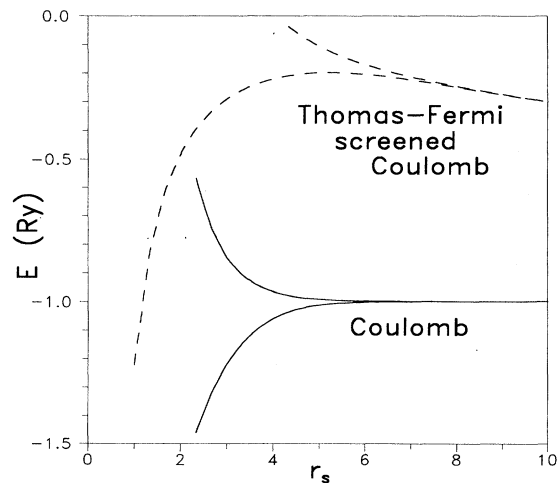


FIG. 1. Result of Wigner-Seitz calculations of the impurity-band bottoms and tops for bare Coulomb and Thomas-Fermi screened Coulomb potentials.

Fermi screened case starts correctly at $E_B = -1$ for $r_s \rightarrow \infty$ and moves rapidly upwards with decreasing r_s . Its absolute energy position is not relevant, a Debye shift^{7,10} was not taken into account and the energy minimum of the continuum states as a function of c was not calculated. Its value is not equal to zero due to the boundary conditions which are different from those of one single Yukawa potential. The crossing of the top of the impurity band with $E = 0$ at $r_s \approx 4$ has nothing to do with the Mott value.

The essential result is that the width of the impurity band calculated in this way is broadened by screening, but remains much smaller than that obtained from the Klauder-V approximation¹¹ (e.g., ≈ 25 times at $r_s = 6.63$ corresponding to $c = N_d = 0.05$ in the notation and units of Ref. 11).

III. THE SMALL CONCENTRATION APPROXIMATION FOR THE SELF-ENERGY

The self-energy for small impurity concentration c has often been calculated (see, e.g., Ref. 34). We shall briefly review here one of these calculations³⁵ in order to provide the basis for subsequent discussions. The equation of motion for the one-particle Green's function under the approximations mentioned in the Introduction (see, e.g., Ref. 35) is

$$G(\mathbf{k}, \mathbf{k}') = G^0(\mathbf{k}, \mathbf{k}') + G^0(\mathbf{k}) \frac{\Omega}{(2\pi)^3} \int d^3\mathbf{q} V(\mathbf{k} - \mathbf{q}) G(\mathbf{q}, \mathbf{k}'), \quad (2)$$

where

$$G^0(\mathbf{k}, \mathbf{k}') = \delta^3(\mathbf{k} - \mathbf{k}') G^0(\mathbf{k})$$

$$\text{with } G^0(\mathbf{k}) = \left[E - \frac{\hbar^2 \mathbf{k}^2}{2m^*} \right]^{-1} \quad (3)$$

is the Green's function for the conduction-band electrons in the effective-mass approximation in the absence of impurities, and

$$V(\mathbf{k}) = \rho(\mathbf{k}) v(\mathbf{k}) \quad (4)$$

is the Fourier transform of the sum of all impurity potentials. The structure factor is given by

$$\rho(\mathbf{k}) = \Omega^{-1} \sum_i e^{-i\mathbf{k} \cdot \mathbf{R}_i}, \quad (5)$$

where the \mathbf{R}_i are the impurity positions and Ω is the total volume. The form factor

$$v(\mathbf{k}) = \int d^3\mathbf{r} V(\mathbf{r}) e^{-i\mathbf{k} \cdot \mathbf{r}} = -\frac{4\pi e^2}{\epsilon} \frac{1}{k^2 + k_{FT}^2} \quad (6)$$

is the Thomas-Fermi screened one-donor Coulomb potential with

$$k_{FT}^2 = \frac{6\pi c e^2}{E_F \epsilon}. \quad (7)$$

The aim is to calculate the configuration averaged Green's function $\bar{G}(\mathbf{k}, \mathbf{k}') = \langle G(\mathbf{k}, \mathbf{k}') \rangle$, where the brackets $\langle \rangle$ denote the average over all possible impurity configurations.

Iterating (2) one obtains

$$\begin{aligned} \bar{G}(\mathbf{k}, \mathbf{k}') &= \delta^3(\mathbf{k} - \mathbf{k}')G^0(\mathbf{k}) + G^0(\mathbf{k})M_1(\mathbf{k} - \mathbf{k}')v(\mathbf{k} - \mathbf{k}')G^0(\mathbf{k}') \\ &+ G^0(\mathbf{k})\frac{\Omega}{(2\pi)^3} \int d\mathbf{k}'' M_2(\mathbf{k} - \mathbf{k}'', \mathbf{k}'' - \mathbf{k}')v(\mathbf{k} - \mathbf{k}'')G^0(\mathbf{k}'')v(\mathbf{k}'' - \mathbf{k}')G^0(\mathbf{k}') + \dots \end{aligned} \quad (8)$$

with

$$M_n(\mathbf{p}_1, \dots, \mathbf{p}_n) = \langle \rho(\mathbf{p}_1) \cdots \rho(\mathbf{p}_n) \rangle. \quad (9)$$

In the case of an uncorrelated impurity distribution the exact cumulant expansion for the M_n is given by³⁵

$$\begin{aligned} M_1(\mathbf{p}_1) &= \langle \rho(\mathbf{p}_1) \rangle_c, \\ M_2(\mathbf{p}_1, \mathbf{p}_2) &= \langle \rho(\mathbf{p}_1) \rangle_c \langle \rho(\mathbf{p}_2) \rangle_c \\ &+ \langle \rho(\mathbf{p}_1) \rho(\mathbf{p}_2) \rangle_c + \dots \end{aligned} \quad (10)$$

with

$$\begin{aligned} \langle \rho(\mathbf{p}_1) \rangle_c &= P_1(c) \delta^3(\mathbf{p}_1) = c \delta^3(\mathbf{p}_1), \\ \langle \rho(\mathbf{p}_1) \rho(\mathbf{p}_2) \rangle_c &= P_2(c) \delta^3(\mathbf{p}_1 + \mathbf{p}_2) \\ &= c(1 - c) \delta^3(\mathbf{p}_1 + \mathbf{p}_2) + \dots \end{aligned} \quad (11)$$

The δ function is normalized so that $\frac{\Omega}{(2\pi)^3} \int d^3k \delta^3(k) = 1$.

A diagrammatic representation of (8) is discussed in Ref. 35. The self-energy then corresponds to the summation of all diagrams of Figs. 2(a)–2(c) with different weights $P_n(c)$ ascribed to the crosses. Retaining only the diagrams of Fig. 2(a) and neglecting nonlinear terms in the $P_n(c)$ we obtain after some algebra the following result, which is correct linear in c :

$$\langle G(\mathbf{k}, \mathbf{k}') \rangle = \delta^3(\mathbf{k} - \mathbf{k}') \bar{G}(\mathbf{k}) \quad (12)$$

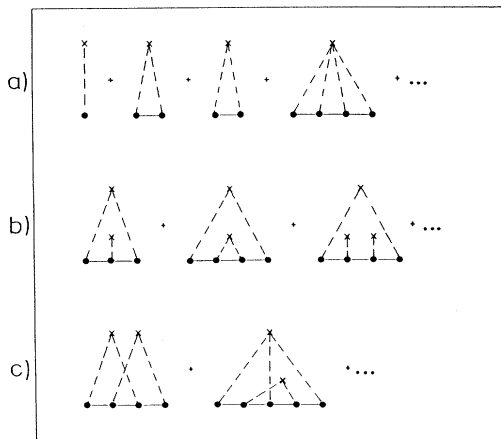


FIG. 2. Diagrams included into the linear approximation (a), the self-consistent approximation (a) and (b), and those neglected in single-site theories (c).

with

$$\bar{G}(\mathbf{k}) = \frac{1}{E - \frac{\hbar^2 \mathbf{k}^2}{2m^*} - M(\mathbf{k}, E)}, \quad (13)$$

where the self-energy $M(\mathbf{k}, E)$ is given by

$$\begin{aligned} M(\mathbf{k}, \mathbf{k}', E) &= \delta^3(\mathbf{k} - \mathbf{k}') M(\mathbf{k}, E) \\ &= c \delta^3(\mathbf{k} - \mathbf{k}') t(\mathbf{k}, \mathbf{k}'; E). \end{aligned} \quad (14)$$

$t(\mathbf{k}, \mathbf{k}'; E)$ is the t matrix of one impurity (multiplied by the total volume Ω) which is given by the integral equation

$$\begin{aligned} t(\mathbf{k}, \mathbf{k}'; E) &= v(\mathbf{k} - \mathbf{k}') \\ &+ \frac{1}{(2\pi)^3} \int d\mathbf{k}'' v(\mathbf{k} - \mathbf{k}'') G^0(\mathbf{k}'') t(\mathbf{k}'', \mathbf{k}'; E). \end{aligned} \quad (15)$$

Hence the self-energy matrix $M(\mathbf{k}, \mathbf{k}', E)$ linear in c is equal to the t matrix of one impurity, multiplied by the concentration and a δ function ensuring momentum conservation. This approximation for the self-energy is identical with the Klauder-IV approximation.²⁵ The calculation of impurity bands is reduced to the solution of the one-impurity problem with subsequent simple numerical calculations to obtain the desired one-particle quantities, such as the densities of states and others, from $M(\mathbf{k}, E)$ or $\bar{G}(\mathbf{k})$ (see, e.g., Ref. 36).

IV. COMPARISON WITH SELF-CONSISTENT THEORIES

In addition to (14) the correct expansion (11) includes diagrams such as those given in Figs. 2(b) and 2(c) with different weights $P_n(c) \neq c$ ascribed to the crosses. These weights are exactly known and correct the diagrams for multiple-occupancy effects (see, e.g., Ref. 34).

However, if diagrams [e.g., those of Fig. 2(c)] are neglected in some approximation, the weights $P_n(c)$ have to be readjusted, otherwise spurious poles occur in \bar{G} (see, e.g., Ref. 34).

The Klauder-V approximation includes all diagrams of Figs. 2(a) and 2(b) but with weights $P_n(c) = c$ neglecting multiple-occupancy corrections. It corresponds to (15) replacing in the kernel of the integral equation $G^0(\mathbf{k})$ by the self-consistent Green's function $\bar{G}(\mathbf{k})$ (13). The intention of the Klauder-V approximation like that of all effective-medium approximations is to include some self-energy terms which are of higher than the first order in c . This, however, with certainty leads to results incorrect linearly in c . The reason is that the linearized solution of a nonlinear algebraic equation is different from the

solution of the linearized equation [e.g., $(M - cA)^2 = 0$ gives $M = cA$, but $M^2 - 2cMA - c^2A^2 \approx M^2 - 2cMA = 0$ gives $M = 0$ and $M = 2cA$]. An effective-medium theory leading to an n th-order equation for M reproduces the correct first-order result (in the concentration) only if all corresponding terms of n th order are taken into account correctly. This, however, is not the case in any effective-medium theory due to the neglect of the diagrams shown in Fig. 2(c). This can be seen easily in the example of δ -like impurity potentials in a conduction band with a Hubbard density³⁷ of states. In this case (see, e.g., Ref. 30) the Klauder-V approximation leads to the self-energy

$$M = -\frac{D}{2} + \frac{cD}{1 - DG^0(E - M)} \quad (16)$$

and the coherent potential approximation²³ as another effective-medium approximation, including multiple occupancy corrections to the diagrams of Figs. 2(a) and 2(b), leads to

$$M = -\frac{D}{2} + \frac{cD}{1 - (\frac{D}{2} - M)G^0(E - M)}. \quad (17)$$

Due to

$$G^0(E - M) = 2[E - M - \sqrt{(E - M)^2 - 1}] \quad (18)$$

in the case of an unperturbed Hubbard density in both cases nonlinear equations (of third order) are obtained for $M(E)$, the solutions of which would be correct linearly in c only if the Taylor expansions (16) or (17) would correctly include all terms $\sim c^2$ and $\sim c^3$.

The reason why this failure leads to a wrong density of states of the impurity band is the following: The self-consistent equation (14) with (15) replacing $G^0(\mathbf{k})$ by $\bar{G}(\mathbf{k})$ in operator form

$$M = cv + v\bar{G}M \quad (19)$$

reproduces the correct result for $c \rightarrow 0$

$$M = cv + vG^0M \quad (20)$$

only if the expansion

$$\bar{G} = G^0 + G^0MG^0 + G^0MG^0MG^0 + \dots \quad (21)$$

converges, which is possible only if the solution M of (20) has no poles as a function of the energy E . Poles of (20), however, correspond just to poles of the one-donor t matrix and hence to the energies of bound states, or to the energies inside the impurity band in the case of a finite impurity concentration. Hence the Klauder-V approximation is incorrect for small c just at the energies of interest. It does not result in the correct boundary condition $\frac{dM}{dc}|_{c=0}$. This incorrectness of effective-medium theories at special energies in the limit $c \rightarrow 0$ was demonstrated numerically for some physical models in Refs. 30 and 31. A detailed investigation, including the subject of the present paper, will be given in a forthcoming paper.³⁸

Because in real semiconductors at all possible donor concentrations a theory linear in c certainly is sufficiently

correct, and because we are mainly interested in the energy range of the impurity band, in which the Klauder-V approximation fails, we will restrict ourselves to the approximation given by (14) and (15) in the subsequent sections.

V. RESULTS

A. Numerical solution

First the integral equation (15) was solved numerically for $\mathbf{k} = 0$ and ∞ , in order to obtain the bottom and the top of the impurity band, discretizing it to a set of linear equations which was solved exactly. We remark that the influence of the electron-electron interaction on the conduction- and the impurity-band positions (see, e.g., Ref. 33) as well as a possible Debye shift (Ref. 10) were not taken into account so that absolute energy values are of no physical relevance here.

The result is shown in Fig. 3. We have chosen the same units as in Ref. 11 (e.g., $c = N_d = \frac{16 \times 9}{\pi^2} r_s^{-3}$) in order to obtain directly comparable results. The resulting bandwidth is much smaller (by a factor of about 5 at $c = 0.05$ corresponding to $r_s = 6.63$) than that obtained in Ref. 11. But it is larger (by a factor of about 5 at $c = 0.05$) than in the case of the Wigner-Seitz calculation (see Fig. 4, too). Both results had been expected: Even without density fluctuations (which are responsible for extended band tails) disorder is expected to broaden bands. The much enhanced bandwidth in the case of a self-consistent theory is due to the failure in reproducing $\frac{dM}{dc}|_{c=0}$ as explained in Sec. III and as obtained in the case of δ -like potentials.³⁰

Higher impurity bands (resulting from $2s, 2p, \dots$ states at $c = 0$) were obtained for small c but are not shown. They rapidly merge with the conduction band with increasing c .

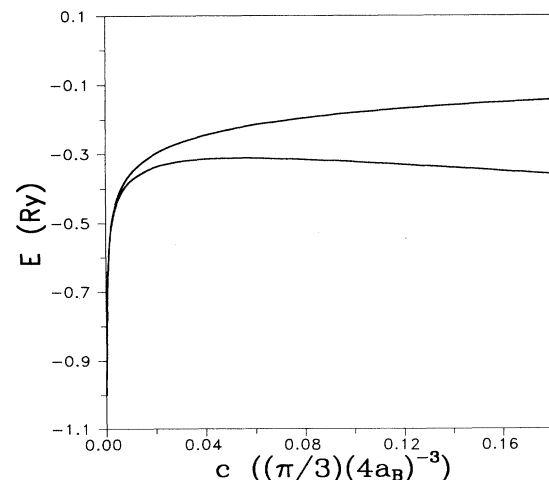


FIG. 3. Impurity-band bottom and top obtained from the numerical solution of the integral equation (15).

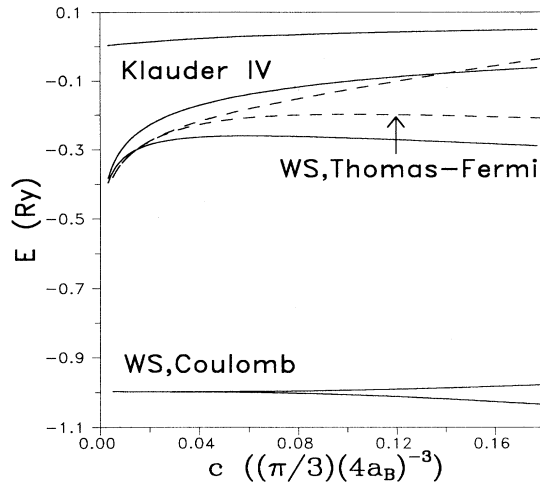


FIG. 4. Impurity-band bottom and top and the conduction-band bottom obtained from the solution of (15) with a separable potential (Klauder-IV approximation), compared with the results of Wigner-Seitz calculations (see Fig. 1).

B. Separable potential approach

Numerical solutions of integral equations are very time consuming and can be avoided with a high degree of accuracy using an artificial technique first applied to our knowledge by Haug and Tran³⁹ and subsequently proved to be applicable to the present problem by Schwabe *et al.*⁴¹ and Gold, Serre, and Ghazali.²⁸ We replace the potential $v(\mathbf{k} - \mathbf{k}')$ by a so-called separable potential

$$v(\mathbf{k} - \mathbf{k}') \rightarrow -v(\mathbf{k})v(\mathbf{k}') \quad (22)$$

with

$$v(\mathbf{k}) = \sqrt{|v(\mathbf{k})|} \bar{b}, \quad (23)$$

choosing b in such a way that in the limit $c \rightarrow 0$ the correct lowest bound state in the potential $v(k)$ is reproduced exactly. In our cases (bare Coulomb and Thomas-Fermi screened Coulomb potential) $b = \frac{1}{2}$ has been examined and finally chosen. We remark that, in principle, b could be chosen to be a function of c in such a way that both the real potential $v(\mathbf{k} - \mathbf{k}')$ and the separable potential $v(\mathbf{k}) \cdot v(\mathbf{k}')$ result, for instance, in the same top of the impurity band. But because absolute energy positions are of no relevance here, we abandoned this possibility.

With the separable potential (22) the integral equation transforms to a simple algebraic equation with the solution

$$M(\mathbf{k}, E) = M(k, E) = -\frac{3}{r_s^3} \frac{1}{k^2 + k_{FT}^2} \frac{1}{1 - \frac{1}{k_{FT} + \sqrt{-E}}}. \quad (24)$$

The result for the impurity band and for the bottom of the conduction band is shown in Fig. 4 together with the results of the Wigner-Seitz calculation. The top of

the impurity band as a function of c comes out to be exactly equal to the energy eigenvalue of one single impurity calculated with the same separable potential. It merges with the conduction band at $c = 1$, corresponding to a Mott value of $r_s = 2.4435$, in good agreement with the experimental value $r_s = 2.386$.⁴⁰ The presence of many impurities simply gives rise to lower states (with $k < \infty$ or $\lambda = \frac{2\pi}{k} > 0$), in which case an electron can be "aware" of the other impurities. The width of the impurity band is nearly the same as in the case of the full potential (Fig. 4) so that we decided (see Ref. 41) to perform all subsequent calculations using the separable potential. Its only lack of applicability seems to be the fact that separable potentials result (for $c \rightarrow 0$) in only one ($1s$ -like) bound state, so that excited impurity bands cannot be obtained, and that absolute energy positions cannot be calculated from them due to the uncertainty in separating $v(0)$.

Figure 5 shows the energies as a function of k for the conduction and impurity bands for different donor concentrations. For $c \rightarrow 0$ or $k \rightarrow \infty$ the impurity band degenerates to a straight line as a function of k as was expected. $E(k)$ is a real function in the impurity band. This is an artifact of the linear approximation (14). The imaginary part of $M(k, E)$ is given by the imaginary part of the t matrix, which has δ -like character at the one-impurity bound states. This is not the case inside the conduction band; the finite lifetimes are indicated in Fig. 5 by dashed lines. In higher orders in c the imaginary part of the self-energy of the impurity band broadens into a Lorentz-like peak even in non-self-consistent theories (see Ref. 30), too.

Figure 6 shows the effective mass m^{**} at the bottom of the impurity band as a function of c . It starts from $m^{**} = \infty$ at $c = 0$ and drops down to a value even smaller

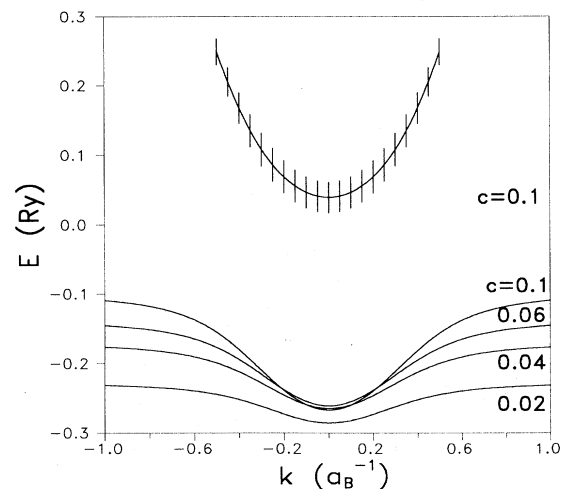


FIG. 5. Dispersion $E(k)$ of the impurity band at different concentrations and the conduction band for $c = 0.1$. The region with $\text{Im}E(k) \neq 0$ of the conduction band extends to $E = 0$. The vertical lines indicate the electron lifetime, the half-width of a Lorentzian approximation to $\text{Im}\bar{G}(k, k, E)$.

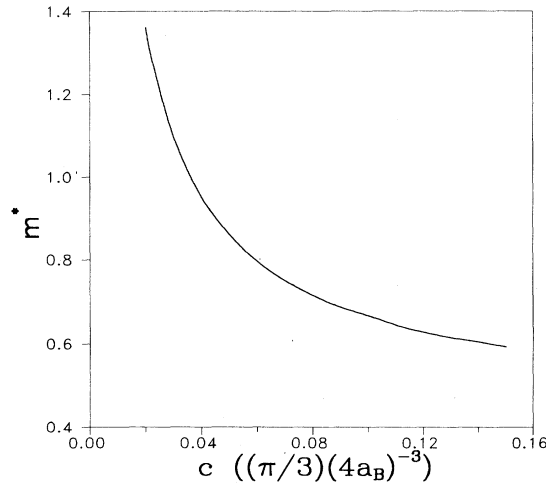


FIG. 6. Concentration dependence of the effective mass m^{**} (in units of m^*) close to the impurity-band bottom.

than the effective mass of the unperturbed conduction band, $m^{**} < m^*$, with increasing c .

The density of states inside the impurity band is plotted for $c = 0.1$ in Fig. 7. It is relatively small near the bottom of the band and becomes infinite at the band top due to the flatness of the $E(k)$ curve for large k (see Fig. 5). This divergency is an artifact of the effective-mass approximation used: replacing the undoped crystal by a homogeneous underground there is no Brillouin zone boundary and the k vector extends to infinity instead of a finite value.

The general behavior of the density of states (smearing out the divergency) bears a close resemblance to the experimental absorption spectra (see, e.g., Ref. 29, the formation of D^-D^+ pairs was not taken into account here) and is strictly dissimilar from the half-egg-like density of states obtained in Ref. 11. The shape of the density of states at the same time clarifies the difference of the bandwidths calculated by either the Wigner-Seitz or by the multiple-scattering approach. Due to the small density of states near the bottom of the impurity band the effective impurity bandwidth is much smaller than its total value shown in Fig. 5.

VI. CONCLUSIONS

We have used both the Wigner-Seitz method and a non-self-consistent multiple-scattering approximation to calculate the electronic structure of impurity bands in

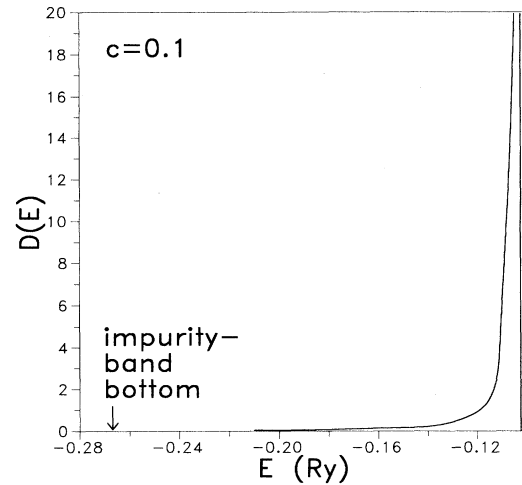


FIG. 7. Density of states of the impurity band obtained from the dispersion $E(k)$ in Fig. 5.

doped semiconductors. We obtained from the non-self-consistent approach a much smaller bandwidth than in the case of a self-consistent approximation¹¹ and traced the difference back to an error of self-consistent theories in the small concentration limit at the energies of interest. The impurity band dispersion $E(k)$ and its density of states, as obtained by us, are much more realistic than those from self-consistent theories and closely resemble experimental line-shape data.²⁹ The same effect was already observed in the cases of δ -like potentials³⁰ and of phonons in mixed crystals.⁴² A very small density of states near the impurity-band bottom at the same time explains remaining differences from the Wigner-Seitz calculations with the same screened potential.

Because we concentrated on the comparison of the non-self-consistent with the self-consistent approach we did not try to improve the simple Thomas-Fermi screening theory using, e.g., a local-density approximation, or to include real many-body effects. Calculating an averaged one-particle Green's function only, we are also not able to obtain extended band tails due to impurity density fluctuations¹²⁻¹⁴ or to obtain knowledge about a possible Anderson localization⁴³ of the impurity-band states.

We restricted ourselves to a three-dimensional impurity distribution. In the case of a two-dimensional arrangement, e.g., in a δ -doping layer,⁴⁴ the problem of a suitable interpolation between a three-dimensional screening in the small concentration limit and a two-dimensional one at high concentrations has to be solved in addition.

¹M. Takeshima, Phys. Rev. B **17**, 3996 (1978).

²T. G. Castner, Philos. Mag. B **42**, 873 (1980).

³G. Röpke and R. Der, Phys. Status Solidi B **92**, 501 (1979).

⁴H. Haug and S. Schmitt-Rink, Prog. Quantum Electron. **9**, 3 (1984).

⁵G. Vignale and W. Hanke, Z. Phys. B **69**, 193 (1987).

⁶G. Vignale, H. Weiler, W. Hanke, and A.A. Maradudin, Z. Phys. B **69**, 209 (1987).

⁷R. Zimmermann, K. Kilimann, W.D. Kraeft, D. Kremp, and G. Röpke, Phys. Status Solidi B **90**, 175 (1978).

⁸G. Röpke, T. Seifert, and K. Kilimann, Ann. Phys. **38**, 381 (1981).

- ⁹K. Kilimann and W. Ebeling, *Z. Naturforsch. A* **45**, 613 (1990).
- ¹⁰J. L. Jackson and L. S. Klein, *Phys. Rev.* **177**, 352 (1969).
- ¹¹J. Serre and A. Ghazali, *Phys. Rev. B* **28**, 4704 (1983).
- ¹²B. I. Halperin and M. Lax, *Phys. Rev.* **148**, 722 (1966); **153**, 802 (1967).
- ¹³J. Zittartz and J. S. Langer, *Phys. Rev.* **148**, 741 (1966).
- ¹⁴I. M. Lifshitz, *Zh. Eksp. Teor. Fiz.* **53**, 743 (1967) [*Sov. Phys. JETP* **26**, 462 (1968)].
- ¹⁵J. Serre, A. Ghazali, and P. Leroux Hugon, *Phys. Rev. B* **23**, 1971 (1981).
- ¹⁶N. F. Mott and J. H. Davies, *Philos. Mag. B* **42**, 845 (1980).
- ¹⁷R. N. Bhatt and T. M. Rice, *Phys. Rev. B* **23**, 1920 (1981).
- ¹⁸J. H. Rose, H. B. Shore, and L. M. Sander, *Phys. Rev. B* **21**, 3037 (1980).
- ¹⁹L. M. Sander, J. R. Rose, and H. B. Shore, *Phys. Rev. B* **21**, 2739 (1980).
- ²⁰E. Wigner and F. Seitz, *Phys. Rev.* **43**, 804 (1933).
- ²¹W. Baltensperger, *Philos. Mag.* **44**, 1355 (1953).
- ²²P. Soven, *Phys. Rev.* **156**, 809 (1967).
- ²³B. Velicky, S. Kirkpatrick, and H. Ehrenreich, *Phys. Rev.* **175**, 747 (1968).
- ²⁴A. Gonig, X.-G. Zhang, and D. M. Nicholson, *Phys. Rev. B* **40**, 947 (1989).
- ²⁵J. R. Klauder, *Ann. Phys. (N.Y.)* **14**, 43 (1961).
- ²⁶A. Ghazali and P. Leroux Hugon, *Phys. Rev. Lett.* **41**, 1569 (1978).
- ²⁷R. Grill, *Phys. Status Solidi B* **162**, 509 (1990).
- ²⁸A. Gold, J. Serre, and A. Ghazali, *Phys. Rev. B* **37**, 4589 (1988).
- ²⁹M. Capizzi, G. A. Thomas, F. De Rosa, R. N. Bhatt, and T. M. Rice, *Solid State Commun.* **31**, 611 (1979).
- ³⁰J. Monecke, *Phys. Status Solidi B* **152**, 123 (1989).
- ³¹J. Monecke, *Phys. Status Solidi B* **155**, 437 (1989).
- ³²C. A. Sholl, *Proc. Phys. Soc.* **92**, 434 (1967).
- ³³K.-F. Berggren and B. E. Sernelius, *Phys. Rev.* **24**, 1971 (1981).
- ³⁴R. J. Elliott, J. A. Krumhansl, and P. L. Leath, *Rev. Mod. Phys.* **46**, 465 (1974).
- ³⁵F. Yonezawa and T. Matsubara, *Prog. Theor. Phys.* **35**, 357 (1966).
- ³⁶J. Monecke, *Phys. Status Solidi B* **153**, 623 (1989).
- ³⁷J. Hubbard, *Proc. R. Soc. London Ser. A* **281**, 401 (1969).
- ³⁸J. Monecke and J. Kortus (unpublished).
- ³⁹H. Haug and D. B. Tran Thoai, *Phys. Status Solidi B* **98**, 581 (1980).
- ⁴⁰P. P. Edwards and M. J. Sienko, *Phys. Rev. B* **17**, 2575 (1978).
- ⁴¹R. Schwabe, A. Haufe, V. Gottschalch, and K. Unger, *Solid State Commun.* **58**, 485 (1986).
- ⁴²J. Monecke, *J. Phys. Condens. Matter* **3**, 4809 (1991).
- ⁴³P. W. Anderson, *Phys. Rev.* **109**, 1492 (1958).
- ⁴⁴G. H. Döhler, *Surf. Sci.* **73**, 97 (1978).